FEBS openbio

CrossMark

Inhibition of malignant phenotypes of human osteosarcoma cells by a gene silencer, a pyrrole–imidazole polyamide, which targets an E-box motif

Masashi Taniguchi [a], Kyoko Fujiwara [b,c,*], Yuji Nakai [d], Toshinori Ozaki [e], Nobuko Koshikawa [f], Kojima Toshio [a], Motoaki Kataba [b], Asako Oguni [b], Hiroyuki Matsuda [c], Yukihiro Yoshida [a], Yasuaki Tokuhashi [a], Noboru Fukuda [b,g], Takahiro Ueno [b,g], Masayoshi Soma [b,c], Hiroki Nagase [f]

[a] Division of Orthopedic Surgery, Nihon University School of Medicine, 30-1 Oyaguchi Kami-Cho, Itabashi, Tokyo 173-8610, Japan
[b] Innovative Therapy Research Group, Nihon University Research Institute of Medical Science, Nihon University School of Medicine, Japan
[c] Division of General Medicine, Department of Internal Medicine, Nihon University School of Medicine, Japan
[d] Graduate School of Agricultural and Life Sciences, The University of Tokyo, Japan
[e] Laboratory of DNA Damage Signaling, Chiba Cancer Center Research Institute, Japan
[f] Laboratory of Cancer Genetics, Chiba Cancer Center Research Institute, Japan
[g] Division of Nephrology, Hypertension and Endocrinology, Department of Medicine, Nihon University School of Medicine, Japan

ARTICLE INFO

ABSTRACT

Gene amplification and/or overexpression of the transcription factor c-MYC, which binds to the E-box sequence (5′-CACGTG-3′), has been observed in many human tumors. In this study, we have designed 5 pyrrole–imidazole (PI) polyamides recognizing E-box, and found that, among them, Myc-6 significantly suppresses malignant phenotypes of human osteosarcoma MG63 cells both in vitro and in vivo. Intriguingly, knockdown of the putative Myc-6 target MALAT1 encoding long noncoding RNA remarkably impaired cell growth of MG63 cells. Collectively, our present findings strongly suggest that Myc-6 exerts its tumor-suppressive ability at least in part through the specific down-regulation of MALAT1.

1. Introduction

Osteosarcoma is the most common primary malignant bone tumor in adolescents and young adults [1]. The curative approach to osteosarcoma includes surgery and chemotherapy. When surgery is not feasible, patients are sometimes subjected to radiotherapy. In the general protocol, 10–12 weeks of neoadjuvant chemotherapy followed by resection and adjuvant chemotherapy is performed to minimize trauma [2]. Although 10-year disease-free survival is around 60% of patients without metastasis, over 30% of the patients suffer metastatic disease at diagnosis [3]. Despite several improvements in the curative protocols, the actual survival trends of osteosarcoma have not been substantially improved over the past 20 years. To overcome the malignant osteosarcoma, the alternative treatments such as hormonal therapy, gene therapy and immune therapy are now under investigation, instead of the conventional chemotherapy, however, the efficacies of those alternative therapeutic strategies are limited and vary among patients [1]. Thus, the development of a novel approach should be required to improve the prognosis of the patients.

MYC family including c-MYC, N-MYC and L-MYC, has been shown to be one of the most frequently altered oncogenes involved in many malignancies. Indeed, the aberrant activation of MYC is detectable in approximately 70% of human cancers [4]. MYC acts as a nuclear sequence-specific transcription factor and exerts its transcriptional activity through the formation of the heterodimeric complex with MAX [5,6]. This MYC/MAX complex specifically binds to the consensus motif termed E-box (5′-CACGTG-3′) and

transactivates its target genes implicated in the crucial cellular processes such as cell cycle regulation, proliferation, metabolism and mitochondrial biogenesis [5].

Amplification of c-*MYC* has been found in musculoskeletal neoplasms including osteosarcoma, chondrosarcoma and soft-tissue sarcoma [7–9]. It has been also shown that c-*MYC* is amplified in several osteosarcoma-derived cell lines, which are sometimes resistant to anti-cancer drugs such as doxorubicin and methotrexate [10]. Notably, knockdown of c-*MYC* resulted in a marked enhancement of sensitivity to cisplatin in osteosarcoma MG63 cells [11]. Since these findings indicate that the amplification of c-*MYC* plays a pivotal role in the regulation of osteosarcoma development and acquisition of chemo-resistance, molecule(s) targeting c-*MYC* and/or E-box might become a novel and attractive chemotherapeutic drug.

Pyrrole–imidazole (PI) polyamides, which have been developed from the DNA-binding antibiotics distamycin A, are small synthetic chemicals composed of the aromatic amino acids N-methylpyrrole (Py) and N-methylimidazole (Im) [12]. According to Dervan's results, PI polyamides bound to the double-strand DNA in a sequence-specific manner and suppressed the transcription of their target genes. A combination of PI polyamides recognized the specific DNA base pairs, (Im/Py, Py/Im and Py/Py pairs bind to G–C, C–G, and A–T/T–A, respectively). A concatenation of these pairs made it possible to bind to a variety of specific DNA sequences. Since PI polyamides were efficiently delivered to cell nuclei without any specific drug-delivery systems, they might be powerful materials to develop gene-specific silencers [13]. Recently, we have generated various types of PI polyamides to down-regulate the expression of their target genes. For example, PI polyamide targeting the consensus activator protein-1 (AP-1)-binding site of the *TGF-β1* promoter significantly inhibited its expression [14]. Additionally, PI polyamide recognizing AP-1-binding site within the promoter of matrix metalloproteinase (MMP)-9 gene markedly reduced its expression level, and thereby strongly inhibiting the migration and invasion of human breast cancer cells in vitro and also abrogating the metastasis in vivo [15].

In this study, we have generated 5 PI polyamides recognizing E-box and found that the PI polyamide termed Myc-6 suppresses the malignant phenotypes of human osteosarcoma MG63 cells at least in part through the specific down-regulation of *MALAT1*.

2. Materials and methods

2.1. Synthesis of PI polyamide targeting E-box

PI polyamides targeting E-box were designed as shown in Fig. 1A and synthesized as described previously [16]. All of the PI polyamides except for Myc-3 were dissolved in distilled water (at a final concentration of 1 mM) and small aliquots were stored at −20 °C. Myc-3 was dissolved in 50% DMSO and small aliquots were kept at −20 °C.

2.2. Cell culture and WST-8 assay

Human osteosarcoma MG63 cells were purchased from Health Science Resource Bank of Japan, and were grown in DMEM (Nakalai) supplemented with 10% of heat-inactivated fetal bovine serum (FBS), 100 μg/mL of streptomycin and 100 units/mL of penicillin. Cultures were maintained at 37 °C in a CO_2 incubator with a controlled humidified atmosphere composed of 95% air and 5% CO_2. Cell proliferation was assessed by WST-8 assay. Cells were seeded at a density of 200 cells/well in 96-well plate and allowed to attach overnight. Cells were then treated with the indicated concentrations of Myc-6. At the indicated time points after the treatment, the

medium was replaced with the fresh medium containing 1/10 volumes of WST-8 reagent, and cells were further incubated for additional 1 h followed by the measurement of absorbance at 450 nm using ARVO MX microplate reader (Perkin Elmer).

2.3. Detection of apoptosis

Apoptosis was detected by using Cell Meter™ Phosphatidylserine Apoptosis assay kit (AAT Bioquest) following the manufacturer's instructions. Briefly, cells were seeded at a density of 400 cells/well in 24-well glass bottom plate, and treated with the indicated concentrations of Myc-6. Following 2 days of the treatment, cells were washed in PBS once, mixed with 500 μl of assay buffer containing Apopxin Violet 500, and incubated for 15 min at room temperature. Cells were examined under a fluorescence microscope (Bravio 9000: KEYENCE) with 470ex/535em.

2.4. Immunoblotting

Cells were washed in PBS and lysed in RIPA buffer. Cell lysates (10 μg of protein) were separated by 10% SDS-polyacrylamide gel electrophoresis and transferred onto Immobilon-P membrane (Millipore). The membrane was blocked with Blocking-one (Nakalai) overnight at 4 °C, and then incubated with anti-caspase-3 (Cell Signaling Technology), anti-cleaved caspase-3 (5A1E: Cell Signaling Technology) or with anti-Actin (AC-15: Sigma) antibody for 1 h at room temperature, followed by the incubation with horseradish peroxidase (HRP)-conjugated secondary antibody (GE Healthcare Life Sciences) for 1 h at room temperature. After washing in PBS containing 0.1% Tween 20, immuno-reactive bands were visualized by using ECL system (Amersham Biosciences) according to the manufacturer's instructions.

2.5. Soft agar colony formation assay

For soft agar assay, cells (5000 cells/plate) were seeded in triplicate in 35-mm cell culture plates containing 0.35% agar and DMEM supplemented with 10% FBS. After 21 days, colonies were stained with crystal violet (WALDECK). Number of colonies with a diameter of > 100 μm was scored. The data shown were the average of 3 independent experiments.

2.6. Mouse xenograft model

Cells (3×10^6 cells) suspended in 200 μl of PBS were injected subcutaneously into the flank of 8-weeks-old male nude mice ($n = 14$). When the tumor volume reached to 200 mm^3, the injection of water or Myc-6 (6 mg/kg body weight) was carried out intravenously and continued once weekly for a total of 4 treatments. Tumor volume was measured once weekly until 5 weeks after the first treatment. All experimental procedures performed on animals were approved by the Laboratory Animal Care Committee of Nihon University School of Medicine.

2.7. Microarray analysis

Cells were plated at a density of 2×10^5 cells/well in 6-well plate, and exposed to 10 μM of Myc-6. Twenty-four hours after the treatment, total RNA was prepared by using TRIZOL reagent (Invitrogen) followed by re-purification with RNAeasy kit (QIAGEN) according to the manufacturer's protocols. Using Total RNA (100 ng), biotin-labeled cRNA probes were synthesized and hybridized to microarrays (Human Genome U133 Plus2.0: Affymetrix) following manufacturer's instructions. The array data (CEL files) were quantified with the distribution free weighted method (DFW) [17] using statistical language R (http://www.r-project)
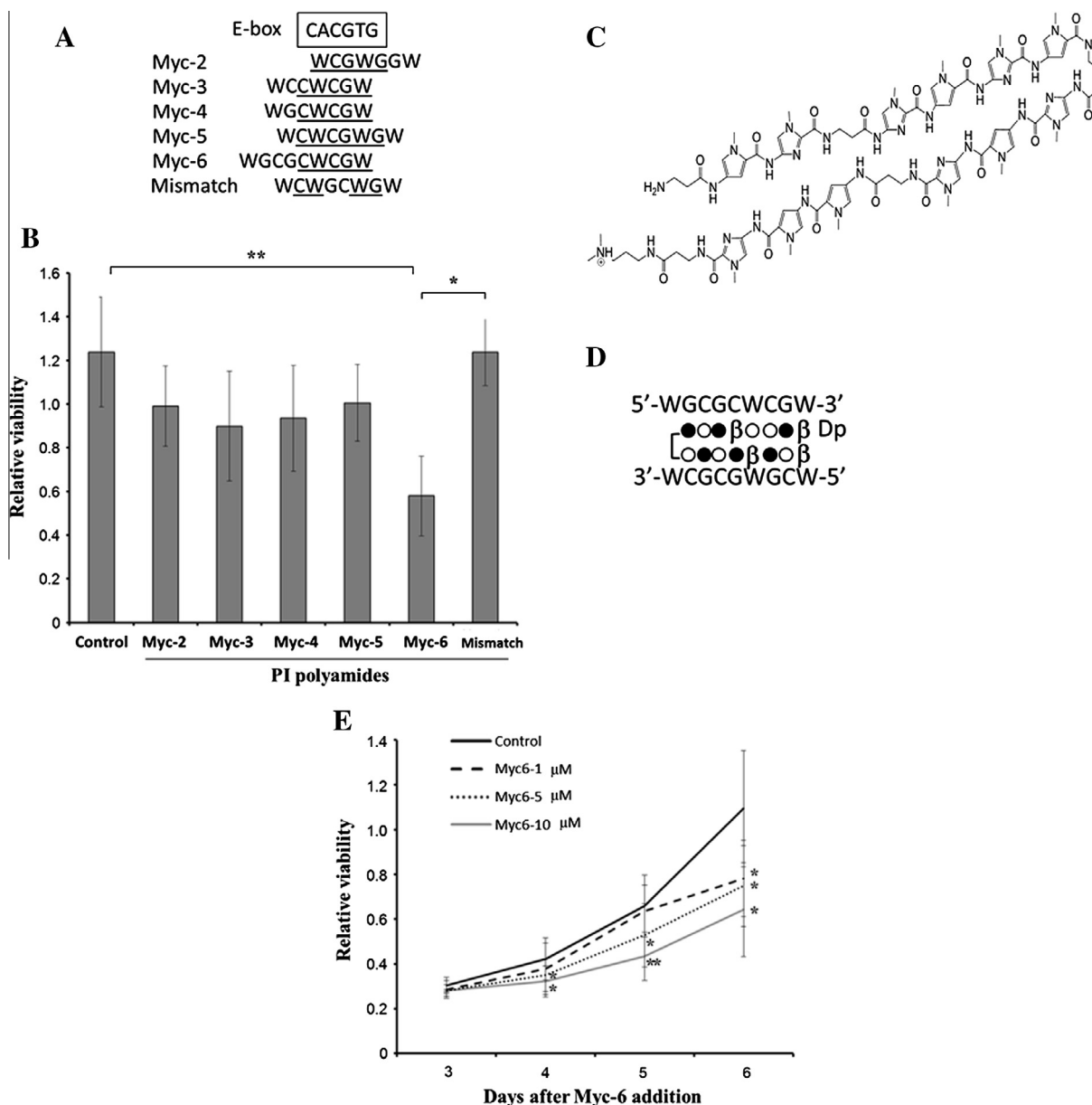
Fig. 1. Myc-6 significantly represses cell viability of human osteosarcoma MG63 cells. (A) Sequence comparison between the putative targets of the indicated synthetic PI polyamides and the consensus E-box. Sequences corresponding to E-box are underlined. W indicates A or T. (B) WST-8 assay. MG63 cells were exposed to water (control), non-specific PI polyamide (mismatch) or with the indicated PI polyamides. Six days after the treatment, cell viability was examined by WST-8 assay. Data are expressed as the means ± SD. Differences were considered significant at $p < 0.05$. $^*p < 0.01$; $^{**}p < 0.001$. (C) Chemical structure of Myc-6. (D) Schematic representation of DNA recognition by Myc-6. Open circle, filled circle, β and Dp indicate pyrrole, imidazole, β-alanine and dimethylpropanediamine, respectively. (E) Dose and time-dependency. Cell viability was measured by WST8 assay 3–6 days after addition of Myc-6. Differences between viability of cells treated with or without Myc-6 were considered significant at $p < 0.05$. $^*p < 0.05$, $^{**}p < 0.01$. Data were expressed as the means ± SD.

[18] and Bioconductor (http://www.bioconductor.org/) [19]. To identify the differentially expressed genes, the rank products method [20] was applied to DFW quantified data. Probe sets with an FDR 0.05 or lower were regarded as having different expression levels between two groups.

2.8. Quantitative real-time PCR

Total RNA was extracted as described above. 500 ng of total RNA were reverse-transcribed using iScript (Bio-Rad). Quantitative real-time PCR was performed using SYBR® Premix ExTaq™ system (Takara). A mixture of cDNA derived from total RNA of MG63 cells treated with or without various amounts of Myc-6 was used as a reference. We then prepared dilution series of this cDNA mixture,

and performed real-time PCR to obtain a standard curve for each gene. Three independent measurements were taken and the amounts were estimated by extrapolation from a standard curve. Expression values were normalized against the expression of β-2-microglobulin and used as an endogenous control. The sequences of the primers used in this study were listed in Supplementary Table 1.

2.9. siRNA-mediated silencing

For Knockdown of *MALAT1*, cells were plated at a density of 200 cells/well in a 96-well plate and allowed to attach overnight. Cells were then transiently transfected with control siRNA or with siRNA against *MALAT1* by using LipofectAMINE RNAiMAX transfec-

tion reagent (Invitrogen) according to the manufacturer's instructions.

2.10. Statistical analysis

All values were expressed as the mean ± SE, and statistical significance was analyzed using the *t*-test. Significance was set at a *p* value of <0.05.

3. Results

3.1. Myc-6-mediated growth suppression of human osteosarcoma MG63 cells

We have designed and generated 5 pyrrole–imidazole (PI) polyamides targeting E-box to suppress malignant phenotypes of cancerous cells (Fig. 1A). Human osteosarcoma MG63 cells were treated with or without these PI polyamides. Six days after the treatment, their cell viability was examined by WST-8 assay. Among 5 PI polyamides examined, Myc-6 significantly inhibited MG63 cell growth and thus we have focused on Myc-6 (Fig. 1B). Schematic drawing of Myc-6 chemical structure and its binding to theoretical target sequence were shown in Fig. 1C and D, respectively. Additional WST assays clearly demonstrated that Myc-6 represses MG63 cell growth in a dose- and time-dependent manner (Fig. 1E).

3.2. MG63 cells undergo apoptosis in response to Myc-6

Since these results indicated that Myc-6 has an ability to prohibit MG63 cell growth, we asked whether Myc-6 could affect the cell cycle distribution. After 72 h of incubation with or without Myc-6, both floating and adherent cells were collected and their cell cycle distribution was examined by Tali image-based cytometer. As seen in Fig. 2A, a dose-dependent massive increase in number of cells with sub-G1 or G1 DNA content was detectable, and also number of cells bearing S phase DNA content was remarkably reduced in a dose-dependent fashion. These observations indicate that MG63 cells undergo apoptosis and/or G1 cell cycle arrest following Myc-6 exposure.

To adequately address this issue, MG63 cells treated with or without Myc-6 were examined by using apopxin violet which monitors the early phase of apoptosis. As shown in Fig. 2B, a dose-dependent marked increase in number of apopxin-positive cells was detectable in response to Myc-6. In contrast, number of apopxin-positive cells was less than 5% without Myc-6. Under the same experimental conditions, cell lysates were prepared and analyzed for the presence of cleaved pro-apoptotic caspase-3 by immunoblotting. As shown in Fig. 2C, the native caspase-3 was detected in cells regardless of Myc-6 treatment, whereas cleaved caspase-3 was detectable in cells exposed to 10 µM of Myc-6. Collectively, our present findings strongly suggest that Myc-6 has an ability to promote apoptosis in MG63 cells.
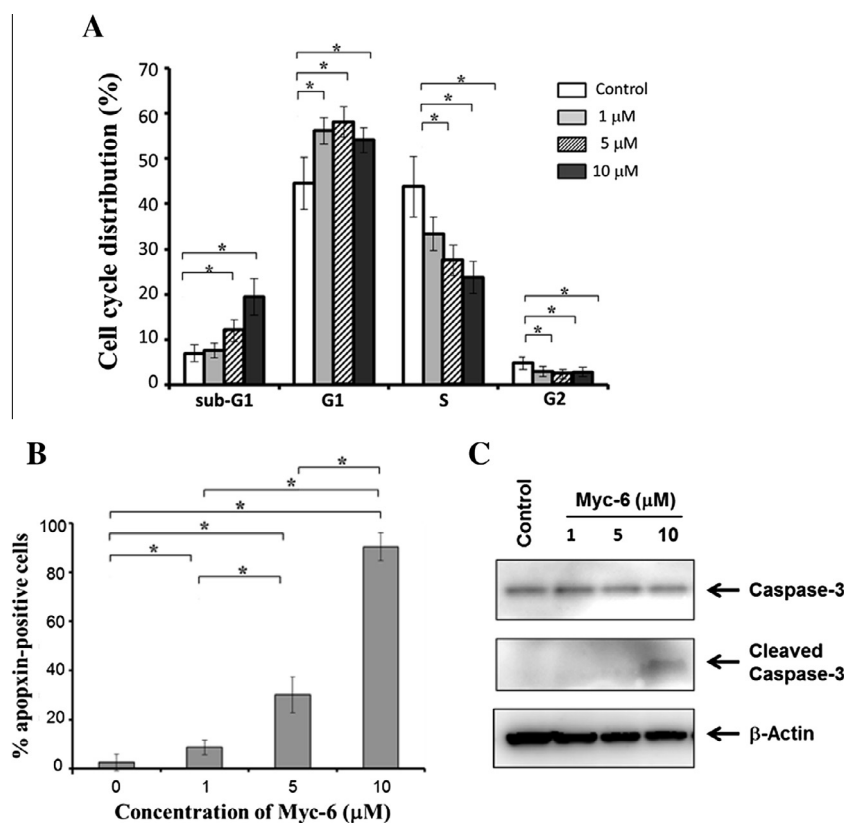

Fig. 2. Myc-6-dependent induction of apoptosis. (A) Tali image-based cytometric analysis. MG63 cells were treated with the indicated concentrations of Myc-6 or left untreated. Following 72 h of Myc-6 exposure, the adherent and attached cells were collected and processed for Tali image-based cytometric analysis. Differences versus cells treated with or without Myc-6 were considered significant at *p* < 0.05. *p < 0.0001. The columns represent means ± SD. (B) Apopxin violet staining. Cells were treated as in (A). Forty-eight hours after the treatment, cells were incubated with apopxin violet 500 solution for 30 min, and then number of apopxin-positive cells was counted. *p < 0.01. (C) Cleavage of pro-apoptotic caspase-3. Cells were treated as in (A). Forty-eight hours after the treatment, cell lysates were prepared and analyzed by immunoblotting with the indicated antibodies.

3.3. Administration of Myc-6 attenuates MG63-derived tumor growth in vivo

Considering that Myc-6 has a potential pro-apoptotic activity, it is likely that Myc-6 might exert tumor-suppressive ability in vitro and in vivo. To address this issue, MG63 cells were plated onto soft agar medium containing the indicated concentrations of Myc-6. Three weeks after the treatment, number of colonies with a diameter of > 100 μm was scored. The number of colonies was significantly decreased in response to 5 or 10 μM of Myc-6 as compared to that of control cells (Fig. 3A), suggesting that Myc-6 prohibits anchorage-independent growth of MG63 cells.

To examine the possible effect of Myc-6 in vivo, we injected MG63 cells subcutaneously into each anterior flank region of athymic nude mice. When tumor volume reached to ∼200 mm³, mice were randomly divided into two groups. Experimental group received 6 mg/kg of Myc-6 intravenously once a week. Control group similarly received water. At the indicated time points after the first administration, tumor volume was measured. Four weeks after the treatment, mice were sacrificed. Consistent with the results obtained from soft agar colony formation assay, a remarkable reduction of tumor volume was observed in Myc-6-treated mice relative to that of control mice (Fig. 3B). The representative pictures were shown in Fig. 3C. These results strongly suggest that Myc-6 possesses tumor-suppressive activity in vivo.

3.4. MALAT1 is a putative Myc-6-target gene

To elucidate the precise molecular mechanism(s) behind Myc-6-mediated induction of apoptosis and suppression of tumor growth, we sought to identify a putative Myc-6-target gene(s) by using DNA microarray-based analysis. After the extensive screening, we have finally obtained 14 genes whose expression levels were significantly lower in Myc-6-treated MG63 cells relative to those in untreated cells (Table 1). The close inspection of their 5′-upstream regions (up to 1 kb) revealed that *MALAT1*, which encodes a long noncoding RNA [21], contains a theoretical Myc-6-tar-
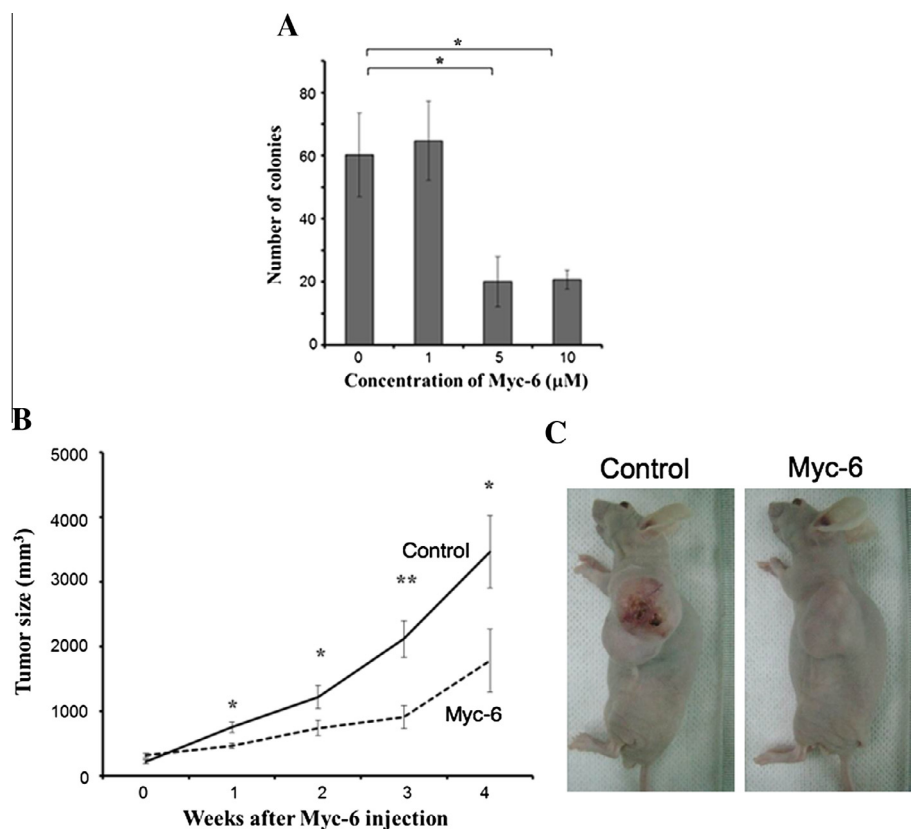
Table 1
List of genes down-regulated by the treatment with Myc-6.

FDR (%)	Gene symbol	Gene name
0.00	NEAT1	Nuclear paraspeckle assembly transcript 1
0.17	DEPDC6	DEP domain containing 6
0.14	NEAT1	Nuclear paraspeckle assembly transcript 1
0.38	COL14A1	Collagen, type XIV, alpha 1
0.40	MALAT1	Metastasis associated lung adenocarcinoma transcript 1
1.00	MMP1	Matrix metallopeptidase 1 (interstitial collagenase)
1.23	RNF145	Ring finger protein 145
1.21	MALAT1	Metastasis associated lung adenocarcinoma transcript 1
1.20	COL3A1	Collagen, type III, alpha 1
1.19	LAMA4	Laminin, alpha 4
2.42	NEAT1	Nuclear paraspeckle assembly transcript 1
2.65	CYP1B1	Cytochrome P450, family 1, subfamily B, polypeptide 1
2.95	C5orf24	Chromosome 5 open reading frame 24
3.67	COL3A1	Collagen, type III, alpha 1
4.04	SFRP1	Secreted frizzled-related protein 1
4.35	ELK4	ELK4, ETS-domain protein (SRF accessory protein 1)
4.22	BE466173	RNA binding motif protein 39
4.86	TAF15	TAF15 RNA polymerase II, TATA box binding protein (TBP)-associated factor

Fig. 3. Tumor-suppressive activity of Myc-6 in vivo. (A) Anchorage-independent growth of MG63 cells. Cells were plated onto soft agar medium containing the indicated concentrations of Myc-6. Three weeks after Myc-6 treatment, number of colonies with a diameter of >100 μM was scored. Differences were considered significant at p < 0.05. *p < 0.01. The columns represent means ± SD. (B and C) Immuno-deficient nude mice bearing subcutaneously developed tumors derived from MG63 cells were injected intravenously with or without Myc-6 (6 μg/kg) once a week. At the indicated time periods after the first injection, tumor volume was measured. p < 0.05 was considered statistically significant. *p < 0.05; **p < 0.01 (B). Representative photographs of tumors were taken 4 weeks after Myc-6 injection (C).
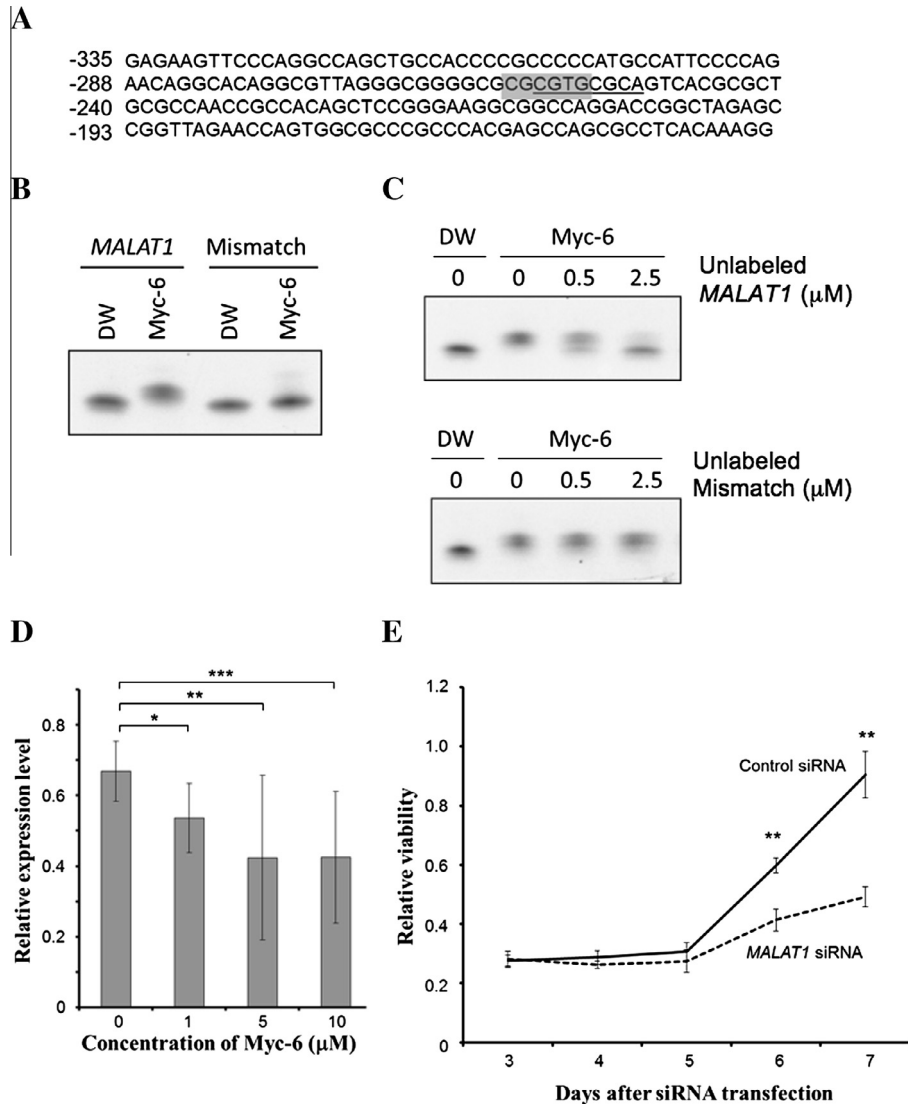
A

```
-335  GAGAAGTTCCCAGGCCAGCTGCCACCCCGCCCCCATGCCATTCCCCAG
-288  AACAGGCACAGGCGTTAGGGCGGGGCGCGCGTGCGCAGTCACGCGCT
-240  GCGCCAACCGCCACAGCTCCGGGAAGGCGGCCAGGACCGGCTAGAGC
-193  CGGTTAGAACCAGTGGCGCCCGCCCACGAGCCAGCGCCTCACAAAGG
```

B

C

D

E

Fig. 4. *MALAT1* is one of possible target genes of Myc-6. (A) Sequence of 5′-upstream region of human *MALAT1* gene. The positions relative to the first nucleotide of *MALAT1* exon 1 (+1) are indicated. The putative Myc-6-target sequence is underlined, and E-box-like sequence is highlighted in gray. (B and C) Gel retardation assay. FITC-labeled specific (*MALAT1*) or non-specific (Mismatch) oligonucleotide (1 μM) was incubated with water or Myc-6 (5 μM) for 1 h at 37 °C. The reaction mixtures were separated by 4–20% gradient polyacrylamide gel electrophoresis and then analyzed by LAS4000 (FUJIFILM) (B). FITC-labeled specific oligonucleotide (0.5 μM) was incubated with Myc-6 (0.5 μM) in the presence or absence of the indicated amounts of unlabeled specific (upper) or non-specific (lower) oligonucleotides. The reaction mixtures were analyzed as in (B) (C). (D) Myc-6-mediated down-regulation of *MALAT1*. MG63 cells were treated with or without the indicated concentrations of Myc-6. Twenty-four hours after treatment, the expression level of *MALAT1* was analyzed by real-time PCR. $p < 0.05$ was considered statistically significant. [*]$p < 0.05$; [**]$p < 0.01$; [***]$p < 0.001$. The columns represent means ± SD. (E) Knockdown of *MALAT1* suppresses MG63 cell growth. MG63 cells were transfected with control siRNA or with siRNA against *MALAT1*. The cell viability was assessed by WST-8 assay. [**]$p < 0.001$.

get sequence including E-box-like motif (at positions −258 to −251) (Fig. 4A). To verify whether Myc-6 could specifically bind to this sequence, we have performed gel retardation assay. FITC-labeled double-strand oligonucleotide corresponding to the above-mentioned *MALAT1* sequence or the unrelated sequence (Mismatch, Supplementary Table 2) was generated, incubated with or without Myc-6 and the reaction mixtures were separated by polyacrylamide gel electrophoresis. Unlike the non-specific oligonucleotide, a definite mobility shift of the specific oligonucleotide was observed in the presence of Myc-6 compared to that in the absence of Myc-6 (Fig. 4B). Furthermore, this mobility shift was clearly inhibited by the excess amount of specific oligonucleotide but not by non-specific one (Fig. 4C), indicating that Myc-6 specifically binds to its theoretical target site located within 5′-upstream region of *MALAT1*.

We then investigated whether Myc-6 could reduce the expression level of *MALAT1 by* real-time PCR. Consistent with the results

obtained from the microarray analysis, Myc-6 exposure led to a dose-dependent decrease in the expression level of *MALAT1* in MG63 cells (Fig. 4D). Finally, we examined whether *MALAT1* could be involved in the regulation of Myc-6-mediated growth suppression by employing siRNA-mediated knockdown of *MALAT1*. MG63 cells were transfected with control siRNA or with siRNA against *MALAT1*. As shown in Fig. 4E, a marked reduction in cell viability was observed in *MALAT1*-knockdown cells relative to that in control cells. Taken together, our present findings strongly suggest that E-box-targeting PI polyamide Myc-6 might exerts its growth- and tumor-suppressive activity at least in part through the specific down-regulation of *MALAT1*.

4. Discussion

In this study, we have found for the first time that Myc-6, a PI polyamide targeting E-box, efficiently suppresses malignant phe-

notypes of human osteosarcoma MG63 cells both in vitro and in vivo, which might be at least in part due to Myc-6-mediated specific down-regulation of *MALAT1*. As expected, *MALAT1* promoter region possessed the theoretical Myc-6-binding sequence containing E-box-like motif. Thus, it is likely that PI polyamide-mediated specific targeting E-box might become an attractive strategy to develop novel anti-tumor drug(s) for the treatment of osteosarcoma.

The development of a small synthetic chemical compound(s), which could block oncogenic signaling pathway, would be ideal as a cancer therapeutic. Several challenges have persisted with respect to drug discovery, including virtual screening of large compound datasets based on computer-aided drug design. Among them, evidence is accumulating that PI polyamide-mediated gene silencing is an alternative and attractive approach to repress malignant phenotypes of tumors [15]. In the current study, we have synthesized 5 PI polyamides targeting E-box according to the general sequence recognition rule for PI polyamides [12]. Among them, Myc-6 displayed an ability to reduce the viability and anchorage-independent growth of MG63 cells in vitro. Moreover, administration of Myc-6 markedly suppressed MG63 cells-derived tumor growth in vivo. Of note, there were no significant changes in body weight between Myc-6-treated and untreated groups of healthy mice, indicating there exists no toxicity of the treatment (data not shown). Additionally, close inspection of their internal organs such as liver, kidney and lung revealed that no morphological changes can be found between them (data not shown). Collectively, it is likely that Myc-6 possesses potential tumor-suppressive function without any severe side effects. However, it should be noted that the remaining 4 PI polyamides examined appear to be biologically insufficient, as no remarkable reduction in cell viability was observed. Although the precise root of this problem has not yet been known, it might be due to their lack of sequence-specificity and/or efficient nuclear access. Further studies should be required to improve the molecular design of PI polyamides.

Another finding of the present study was that *MALAT1* encoding a long noncoding RNA might be one of Myc-6-target genes. Consistent with our observations, it has been shown that *MALAT1* is up-regulated in several human solid tumors and its aberrant higher expression level is tightly linked to tumor metastasis and recurrence [22]. Notably, forced expression of *MALAT1* enhanced tumor formation in nude mice, while depletion of *MALAT1* in cancerous cells reduced their tumorigenicity [23]. These findings suggest that *MALAT1* has an oncogenic function, however, the precise molecular basis has been elusive. Recently Tripathi et al. described that depletion of *MALAT1* leads to an induction of tumor suppressor p53 along with its targets such as *p21^{WAF1}* and *GADD45*, indicating that p53 and/or another p53 family members such as p73 might be a downstream mediator of *MALAT1* [24]. Further experiments should be required to adequately address how *MALAT1* could contribute to Myc-6-dependent tumor suppression.

Conflict of interest

The authors declare no conflict of interest.

Acknowledgements

Appendix A. Supplementary data

Supplementary data associated with this article can be found, in the online version, at http://dx.doi.org/10.1016/j.fob.2014.03.004.

References

[1] Tan, M.L., Choong, P.F. and Dass, C.R. (2009) Osteosarcoma: conventional treatment vs. gene therapy. Cancer Biol. Ther. 8, 106–117.
[2] Gill, J., Ahluwalia, M.K., Geller, D. and Gorlick, R. (2013) New targets and approaches in osteosarcoma. Pharmacol. Ther. 137, 89–99.
[3] Longhi, A., Errani, C., De, P.M., Mercuri, M. and Bacci, G. (2006) Primary bone osteosarcoma in the pediatric age: state of the art. Cancer Treat. Rev. 32, 423–436.
[4] Nilsson, J.A. and Cleveland, J.L. (2003) Myc pathways provoking cell suicide and cancer. Oncogene 22, 9007–9021.
[5] Dang, C.V. (2012) MYC on the path to cancer. Cell 149, 22–35.
[6] Cascon, A. and Robledo, M. (2012) MAX and MYC: a heritable breakup. Cancer Res. 72, 3119–3124.
[7] Barrios, C., Castresana, J.S., Ruiz, J. and Kreicbergs, A. (1993) Amplification of c-myc oncogene and absence of c-Ha-ras point mutation in human bone sarcoma. J. Orthop. Res. 11, 556–563.
[8] Ladanyi, M., Park, C.K., Lewis, R., Jhanwar, S.C., Healey, J.H. and Huvos, A.G. (1993) Sporadic amplification of the MYC gene in human osteosarcomas. Diagn. Mol. Pathol. 2, 163–167.
[9] Barrios, C., Castresana, J.S., Falkmer, U.G., Rosendahl, I. and Kreicbergs, A. (1994) C-myc oncogene amplification and cytometric DNA ploidy pattern as prognostic factors in musculoskeletal neoplasms. Int. J. Cancer 58, 781–786.
[10] Hattinger, C.M., Stoico, G., Michelacci, F., Pasello, M., Scionti, I., Remondini, D., Castellani, G.C., Fanelli, M., Scotlandi, K., Picci, P. and Serra, M. (2009) Mechanisms of gene amplification and evidence of coamplification in drug-resistant human osteosarcoma cell lines. Genes Chromosomes. Cancer 48, 289–309.
[11] Xie, X.K., Yang, D.S., Ye, Z.M. and Tao, H.M. (2009) Enhancement effect of adenovirus-mediated antisense c-myc and caffeine on the cytotoxicity of cisplatin in osteosarcoma cell lines. Chemotherapy 55, 433–440.
[12] Dervan, P.B. and Edelson, B.S. (2003) Recognition of the DNA minor groove by pyrrole–imidazole polyamides. Curr. Opin. Struct. Biol. 13, 284–299.
[13] Murty, M.S. and Sugiyama, H. (2004) Biology of N-methylpyrrole-N-methylimidazole hairpin polyamide. Biol. Pharm. Bull. 27, 468–474.
[14] Matsuda, H., Fukuda, N., Ueno, T., Katakawa, M., Wang, X., Watanabe, T., Matsui, S., Aoyama, T., Saito, K., Bando, T., Matsumoto, Y., Nagase, H., Matsumoto, K. and Sugiyama, H. (2011) Transcriptional inhibition of progressive renal disease by gene silencing pyrrole–imidazole polyamide targeting of the transforming growth factor-beta1 promoter. Kidney Int. 79, 46–56.
[15] Wang, X., Nagase, H., Watanabe, T., Nobusue, H., Suzuki, T., Asami, Y., Shinojima, Y., Kawashima, H., Takagi, K., Mishra, R., Igarashi, J., Kimura, M., Takayama, T., Fukuda, N. and Sugiyama, H. (2010) Inhibition of MMP-9 transcription and suppression of tumor metastasis by pyrrole–imidazole polyamide. Cancer Sci. 101, 759–766.
[16] Bando, T. and Sugiyama, H. (2006) Synthesis and biological properties of sequence-specific DNA-alkylating pyrrole–imidazole polyamides. Acc. Chem. Res. 39, 935–944.
[17] Chen, Z., McGee, M., Liu, Q. and Scheuermann, R.H. (2007) A distribution free summarization method for Affymetrix GeneChip arrays. Bioinformatics 23, 321–327.
[18] R development core team (2006) R: A language and environment for statistical computing, R foundation for statistical computing, Vienna, Austria.
[19] Gentleman, R.C., Carey, V.J., Bates, D.M., Bolstad, B., Dettling, M., Dudoit, S., Ellis, B., Gautier, L., Ge, Y., Gentry, J., Hornik, K., Hothorn, T., Huber, W., Iacus, S., Irizarry, R., Leisch, F., Li, C., Maechler, M., Rossini, A.J., Sawitzki, G., Smith, C., Smyth, G., Tierney, L., Yang, J.Y. and Zhang, J. (2004) Bioconductor: open software development for computational biology and bioinformatics. Genome Biol. 5, R80.
[20] Breitling, R., Armengaud, P., Amtmann, A. and Herzyk, P. (2004) Rank products: a simple, yet powerful, new method to detect differentially regulated genes in replicated microarray experiments. FEBS Lett. 573, 83–92.
[21] Ji, P., Diederichs, S., Wang, W., Boing, S., Metzger, R., Schneider, P.M., Tidow, N., Brandt, B., Buerger, H., Bulk, E., Thomas, M., Berdel, W.E., Serve, H. and Muller-Tidow, C. (2003) MALAT-1, a novel noncoding RNA, and thymosin beta4 predict metastasis and survival in early-stage non-small cell lung cancer. Oncogene 22, 8031–8041.
[22] Gutschner, T. and Diederichs, S. (2012) The hallmarks of cancer: a long non-coding RNA point of view. RNA Biol. 9, 703–719.
[23] Schmidt, L.H., Spieker, T., Koschmieder, S., Schaffers, S., Humberg, J., Jungen, D., Bulk, E., Hascher, A., Wittmer, D., Marra, A., Hillejan, L., Wiebe, K., Berdel, W.E., Wiewrodt, R. and Muller-Tidow, C. (2011) The long noncoding MALAT-1 RNA indicates a poor prognosis in non-small cell lung cancer and induces migration and tumor growth. J. Thorac. Oncol. 6, 1984–1992.
[24] Tripathi, V., Shen, Z., Chakraborty, A., Giri, S., Freier, S.M., Wu, X., Zhang, Y., Gorospe, M., Prasanth, S.G., Lal, A. and Prasanth, K.V. (2013) Long noncoding RNA MALAT1 controls cell cycle progression by regulating the expression of oncogenic transcription factor B-MYB. PLoS Genet. 9, e1003368.